



HAL
open science

A finite element based stability test for equilibria of flexible structures in circular orbits

Wolfgang Steiner

► **To cite this version:**

Wolfgang Steiner. A finite element based stability test for equilibria of flexible structures in circular orbits. *International Journal of Non-Linear Mechanics*, 2008, 43 (7), pp.650. 10.1016/j.ijnonlinmec.2008.03.004 . hal-00501782

HAL Id: hal-00501782

<https://hal.science/hal-00501782>

Submitted on 12 Jul 2010

HAL is a multi-disciplinary open access archive for the deposit and dissemination of scientific research documents, whether they are published or not. The documents may come from teaching and research institutions in France or abroad, or from public or private research centers.

L'archive ouverte pluridisciplinaire **HAL**, est destinée au dépôt et à la diffusion de documents scientifiques de niveau recherche, publiés ou non, émanant des établissements d'enseignement et de recherche français ou étrangers, des laboratoires publics ou privés.

Author's Accepted Manuscript

A finite element based stability test for equilibria of flexible structures in circular orbits

Wolfgang Steiner

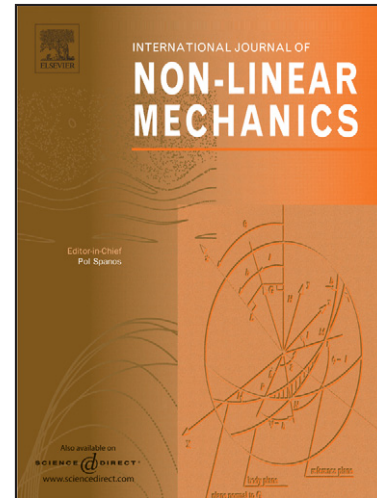
PII: S0020-7462(08)00047-4
DOI: doi:10.1016/j.ijnonlinmec.2008.03.004
Reference: NLM 1457

To appear in: *International Journal of Non-Linear Mechanics*

Received date: 9 August 2007
Revised date: 3 March 2008
Accepted date: 5 March 2008

Cite this article as: Wolfgang Steiner, A finite element based stability test for equilibria of flexible structures in circular orbits, *International Journal of Non-Linear Mechanics* (2008), doi:10.1016/j.ijnonlinmec.2008.03.004

This is a PDF file of an unedited manuscript that has been accepted for publication. As a service to our customers we are providing this early version of the manuscript. The manuscript will undergo copyediting, typesetting, and review of the resulting galley proof before it is published in its final citable form. Please note that during the production process errors may be discovered which could affect the content, and all legal disclaimers that apply to the journal pertain.



www.elsevier.com/locate/nlm

A Finite Element Based Stability Test for Equilibria of Flexible Structures in Circular Orbits

Wolfgang Steiner

*University of Applied Sciences Upper Austria
Stelzhamerstr. 23, A-4600 Wels
Tel.: +43-72811-3230
Fax: +43-72811-3166
wsteiner@fh-wels.at*

Abstract

Large flexible structures could be one of the most challenging space technologies of the future. For example, the well known *space elevator* may one day guide astronauts along a 36,000 km long tether from the earth's surface to a geostationary orbit. In this paper, we imagine an arbitrary space structure in a stationary circular motion around a celestial body.

Usually such systems require two problems to be solved: the strength of the materials and an overall stability analysis. The latter task is a non-trivial one since in orbiting systems not the angular rate, but the angular momentum must be kept constant when applying, for example, Dirichlet's criterion. In particular, this fact becomes important if the system's dimension is in the magnitude of the orbital radius. Therefore, this paper will focus on a general applicable method to determine the stability of flexible earth orbiting structures.

The analysis process is based on the *reduced energy momentum method* presented by J. C. Simo, T. A. Posbergh and J. E. Marsden, which has been customized for use in systems with cyclic coordinates by the author. In the presented approach the second variation of an *amended potential* is derived from a standard finite element analysis. An efficient stability test is introduced which limits the computational effort to the evaluation of a few eigenvalues and eigenvectors of the system's tangent stiffness matrix. Finally, two examples are discussed to demonstrate the application of the method.

Key words: Stability, Nonlinear Mechanical System, Relative Equilibrium, Finite Elements, Amended Potential, Space Elevator, Reduced Energy Momentum Method

1 Introduction

Many technical systems operate in a so-called *relative equilibrium configuration*, which is characterized by the fact that the only dynamic process is a uniform motion in a symmetry group like a rotation about an axis at a constant angular rate. For example, consider a rotating turbine or a spacecraft in a stationary circular motion around a celestial body. To find a relative equilibrium for such systems one usually introduces a properly rotating reference frame in which the field of centrifugal forces acts as an external load. If the system consists of flexible bodies finite element programs can then be used to compute deformations and stresses by carrying out a standard static analysis.

However, for technical applications it is also necessary to analyze the stability of a relative equilibrium. For example, it is known that large space structures may become unstable, if the system's dimension is in the magnitude of the orbital radius. Here one must always take care about the fact that for a perturbation motion of a relative equilibrium not the velocity of the group parameter but the corresponding momentum is conserved. Therefore, in the case of a rotating system the angular velocity must not be treated as a constant quantity.

In this paper a general stability test for flexible orbiting structures is presented, taking into account the correct conservation of the angular momentum. The test employs the method of the *amended potential* presented in [(5)] and [(4)] which has also been derived in [(7)] from an engineer's point of view. It can be applied as a post-processing step at the end of a standard finite element analysis and is also suitable for systems with many degrees of freedom since the computational effort is minimized by a proper decomposition of the second derivatives of the amended potential. Thus, only the eigenvalues and eigenvectors of the tangent stiffness matrix and the load vector of the centrifugal forces for the relative equilibrium are required as input for the test.

To demonstrate how the test works, the stability of a so-called *space elevator* is analyzed. One day this structure could enable astronauts to climb up a 36,000 km long tether connecting the earth's surface with a geostationary orbit. However, it turns out that an orbiting tether becomes unstable beyond a critical length [(7), (6)].

2 Stability of relative equilibria

We briefly recall the results of the stability analysis process described in [(7)]. A relative equilibrium is closely related to the existence of *cyclic coordinates*,

i.e. generalized coordinates that do not appear explicitly in the Lagrangian. In a relative equilibrium these coordinates vary uniformly like the rotation angle of a rotating system. Conversely, the non-cyclic coordinates remain stationary during the motion.

Let \mathbf{q}_c and \mathbf{q}_n be the vectors of the cyclic and the non-cyclic coordinates. The kinetic energy of the system is then given by

$$T = \frac{1}{2} \dot{\mathbf{q}}^\top \mathbf{M}(\mathbf{q}_n) \dot{\mathbf{q}} = \frac{1}{2} \begin{pmatrix} \dot{\mathbf{q}}_c^\top & \dot{\mathbf{q}}_n^\top \end{pmatrix} \begin{pmatrix} \mathbf{M}_{cc} & \mathbf{M}_{cn} \\ \mathbf{M}_{nc} & \mathbf{M}_{nn} \end{pmatrix} \begin{pmatrix} \dot{\mathbf{q}}_c \\ \dot{\mathbf{q}}_n \end{pmatrix} \quad (1)$$

introducing $\mathbf{M}(\mathbf{q}_n)$ as the mass matrix. For the stability analysis only the submatrix \mathbf{M}_{cc} , known as *locked inertia tensor*, is needed. It is derived from the mechanical model by setting the velocities of the non-cyclic coordinates $\dot{\mathbf{q}}_n$ to zero and $\dot{\mathbf{q}}_c = \omega = \text{const}$. In this case the kinetic energy reads

$$T_c = \frac{1}{2} \omega^\top \mathbf{M}_{cc}(\mathbf{q}_n) \omega. \quad (2)$$

Now, since $\dot{\mathbf{q}}_c$ is a cyclic coordinate, the corresponding generalized momentum

$$\mathbf{p}_c = \frac{\partial T}{\partial \dot{\mathbf{q}}_c} = \mathbf{M}_{cc}(\mathbf{q}_n) \omega \quad (3)$$

is a first integral of the system and will therefore be conserved. This must be taken into account when disturbing a relative equilibrium in order to check its stability.

In Steiner [(7)] it is shown that relative equilibria and the correct stability test can be derived from the *amended potential*

$$V^*(\mathbf{q}_n) = \frac{1}{2} \mathbf{p}_c^\top \mathbf{M}_{cc}^{-1} \mathbf{p}_c + V(\mathbf{q}_n) \quad (4)$$

where $V(\mathbf{q}_n)$ is the physical potential energy (depending on \mathbf{q}_n only). A set of nonlinear equations for the equilibrium configuration of the non-cyclic coordinates is obtained from

$$\frac{\partial V^*}{\partial \mathbf{q}_n} = 0 \quad \text{at} \quad \mathbf{q}_n = \mathbf{q}_{n,0}. \quad (5)$$

Furthermore, the equilibrium is stable if the matrix of second derivatives of V^*

$$A_{ij} = \frac{\partial^2 V^*}{\partial q_n^i \partial q_n^j} \quad (6)$$

is positive definite at $\mathbf{q}_n = \mathbf{q}_{n,0}$. We point out, that for all derivatives in (5) and (6) \mathbf{p}_c must be kept constant. Therefore, it is strictly forbidden to insert (3) into (4) *before* carrying out these operations.

3 Modelling an orbiting flexible structure with finite elements

Let us consider now an arbitrary flexible structure rotating around a celestial body. Usually one introduces a rotating reference frame as depicted in fig. 1 to describe (relative) equilibrium configurations of the structure, since no time-dependent coordinates will appear in this case. We can define the reference frame by a selected point that is constrained to the y-z-plane ($x = 0$). In fig. 1 this point is labelled "Node 1". Additionally, the z-Axis is fixed in the inertial frame.

Next we introduce a finite element discretization for the flexible structure. Then the equilibrium configuration is described by a vector $\mathbf{u} \in \mathbb{R}^N$ of nodal degrees of freedom representing translations and rotations of the nodes with respect to an unstressed reference configuration. If we only include the unconstrained degrees of freedom in \mathbf{u} , then this vector represents the non-cyclic coordinates of the system, i. e. $\mathbf{q}_n = \mathbf{u}$. Note that the translation of node 1 along the x-axis is not an element of \mathbf{u} since this degree of freedom is locked in order to define the reference frame.

Now, to describe the configuration of the structure in an inertial frame we have to consider the rotation angle φ of the reference frame as an additional variable. In a relative equilibrium φ is a uniformly varying quantity, i. e.

$$\dot{\varphi} = \omega = \text{const.} \quad (7)$$

Therefore, φ is the cyclic variable of the system.

Moreover, since $q_c = \varphi$ is the *only* cyclic variable, the locked inertia tensor \mathbf{M}_{cc} is a scalar M_{cc} which depends on the non-cyclic coordinates \mathbf{u} . As described in (2) it can be derived from the kinetic energy for $\dot{\mathbf{u}} = 0$. Since the system rotates around the z-axis we obtain

$$T_c = \frac{1}{2} \int_m v^2 dm = \frac{1}{2} \int_m (\omega r_z)^2 dm = \frac{1}{2} \omega^2 \int_m (x^2 + y^2) dm \quad (8)$$

where x and y denote the x- and y-coordinate of a mass element dm in the deformed configuration. Comparing (8) with (2) we get

$$M_{cc} = \int_m (x^2 + y^2) dm \quad (9)$$

where x and y can be expressed by \mathbf{u} and the ansatz-functions introduced for the discretization process. Physically speaking, $M_{cc} = M_{cc}(\mathbf{u})$ is the moment of inertia about the z-axis for a configuration \mathbf{u} .

To describe the dynamic behaviour of our system the potential energy $V(\mathbf{u})$ must be known. It consists of two parts, the strain energy U and the potential

of the external load V_G . The strain energy is the key functional used in finite element solvers for the derivation of "internal nodal forces". The external load of space vehicles is usually dominated by gravitational forces. Let κ be the gravitational parameter of the celestial body, then

$$V_G = - \int_m \frac{\kappa}{r} dm = - \int_m \frac{\kappa}{\sqrt{x^2 + y^2 + z^2}} dm. \quad (10)$$

Again, for numerical solutions x , y and z must be discretized by proper ansatz-functions. Since not all software products allow the implementation of gravitational forces, it may become necessary to write user subroutines to take into account this type of loading, see section 6.

From the discretized functionals M_{cc} and $V = U + V_G$ the amended potential (4) can be derived:

$$V^*(\mathbf{u}) = V(\mathbf{u}) + \frac{1}{2} \frac{p_c^2}{M_{cc}(\mathbf{u})}. \quad (11)$$

Here, p_c is the conserved angular momentum

$$p_c = M_{cc}(\mathbf{u})\omega \quad (12)$$

which must be treated as a constant parameter in (11). Note, that all matrix products in (3) and (4) are reduced to simple one-dimensional operations in (11) and (12) since φ is the only cyclic variable.

Using the amended potential, the equations, which determine the relative equilibria $\mathbf{u} = \mathbf{u}^0$, read

$$\frac{\partial V^*}{\partial \mathbf{u}} = \frac{\partial V}{\partial \mathbf{u}} - \frac{1}{2} \frac{p_c^2}{M_{cc}^2} \frac{\partial M_{cc}}{\partial \mathbf{u}} = \mathbf{0}. \quad (13)$$

In these equations the expression

$$\mathbf{f}_c = \frac{1}{2} \frac{p_c^2}{M_{cc}^2} \frac{\partial M_{cc}}{\partial \mathbf{u}} = \frac{1}{2} \omega^2 \frac{\partial M_{cc}}{\partial \mathbf{u}} \quad (14)$$

is the load vector of centrifugal forces acting on the structure in the rotating reference frame. Most finite element solvers allow this type of load to be applied for a given ω . It is also easy to extract this vector from the FE-solver. For example, after computing the equilibrium in the first analysis step one can switch off the centrifugal loading while suppressing further nodal displacements in a subsequent step. The vector of nodal reaction forces (and moments) will then contain the elements of \mathbf{f}_c .

Proceeding from the amended potential we are now ready to analyze the stability of the relative equilibrium. To build up the matrix of second derivatives of V^* the left side of (13) must be differentiated once more. Keeping p_c constant

we obtain

$$A_{ij} = \frac{\partial^2 V^*}{\partial u_i \partial u_j} = \frac{\partial^2 V}{\partial u_i \partial u_j} - \frac{1}{2} \frac{p_c^2}{M_{cc}^2} \frac{\partial^2 M_{cc}}{\partial u_i \partial u_j} + \frac{p_c^2}{M_{cc}^3} \frac{\partial M_{cc}}{\partial u_i} \frac{\partial M_{cc}}{\partial u_j}. \quad (15)$$

Note that the last term would disappear if ω instead of p_c were kept constant. However, we may substitute $p_c = M_{cc}\omega$ in (15) to describe A_{ij} in terms of ω :

$$A_{ij} = \frac{\partial^2 V}{\partial u_i \partial u_j} - \frac{1}{2} \omega^2 \frac{\partial^2 M_{cc}}{\partial u_i \partial u_j} + \frac{\omega^2}{M_{cc}} \frac{\partial M_{cc}}{\partial u_i} \frac{\partial M_{cc}}{\partial u_j}. \quad (16)$$

If the system is stable the matrix $\mathbf{A} = \{A_{ij}\}$ must be positive definite for $\mathbf{u} = \mathbf{u}^0$.

4 Stability analysis

It is the main goal of this paper to derive a simple stability test for flexible orbiting structures from (16), which uses only data available from a standard finite element analysis. Therefore, we note that A_{ij} separates into two parts.

First, the matrix

$$K_{ij} = \frac{\partial^2 V}{\partial u_i \partial u_j} - \frac{1}{2} \omega^2 \frac{\partial^2 M_{cc}}{\partial u_i \partial u_j} \quad (17)$$

is the tangent stiffness matrix of the system for a constant rotation of the reference frame. It includes all structural stiffness effects as well as load stiffness contributions due to centrifugal and gravitational forces. The FE-software also uses this matrix to solve for equilibrium configurations by means of the Newton-Raphson method. It can be exported from most FE-programs. However, we shall see that this is not necessary.

The latter part of (16)

$$\frac{\omega^2}{M_{cc}} \frac{\partial M_{cc}}{\partial u_i} \frac{\partial M_{cc}}{\partial u_j} = \left(\frac{\omega}{\sqrt{M_{cc}}} \frac{\partial M_{cc}}{\partial u_i} \right) \left(\frac{\omega}{\sqrt{M_{cc}}} \frac{\partial M_{cc}}{\partial u_j} \right) \quad (18)$$

is the tensor product of the vector

$$\mathbf{a} = \frac{\omega}{\sqrt{M_{cc}}} \frac{\partial M_{cc}}{\partial \mathbf{u}} = \frac{\omega}{\sqrt{M_{cc}}} \frac{2}{\omega^2} \mathbf{f}_c = \sqrt{\frac{4}{M_{cc}\omega^2}} \mathbf{f}_c = \sqrt{\frac{2}{T_c}} \mathbf{f}_c \quad (19)$$

where we have used (14) and (2), i. e. $T_c = M_{cc}\omega^2/2$.

With (17), (18) and (19) we may now rewrite (16) in the following way:

$$A_{ij} = K_{ij} + a_i a_j \quad \iff \quad \mathbf{A} = \mathbf{K} + \mathbf{a} \mathbf{a}^T \quad (20)$$

Here, the matrix notation $\mathbf{a}\mathbf{a}^\top = \mathbf{a} \otimes \mathbf{a}$ was used to express the tensor product. \mathbf{A} is positive definite, if the quadratic form

$$\mathbf{x}^\top \mathbf{A} \mathbf{x} = \mathbf{x}^\top (\mathbf{K} + \mathbf{a}\mathbf{a}^\top) \mathbf{x} \quad (21)$$

is positive for an arbitrary vector $\mathbf{x} \in \mathbb{R}^N$ and zero only for $\mathbf{x} = \mathbf{0}$. In this case, the system is stable.

Now, to show that \mathbf{A} is positive definite we could simply compute the lowest eigenvalue of \mathbf{A} and see if it is positive. However, \mathbf{A} contains a tensor product and is therefore a dense matrix. For large FE-models the eigenvalue extraction of \mathbf{A} may cause difficulty. On the other hand, the tangent stiffness matrix \mathbf{K} is a sparse matrix for which eigenvectors and eigenvalues can be extracted efficiently.

Let $\lambda_1, \dots, \lambda_N$ be the eigenvalues of \mathbf{K} sorted by its magnitude, i. e. $\lambda_1 < \lambda_2 < \dots < \lambda_N$, and let $\mathbf{v}_1, \dots, \mathbf{v}_N$ be the corresponding eigenvectors of \mathbf{K} . (For example, these objects can be obtained from FE-solvers by performing a natural frequency extraction, if the mass matrix is set to the unity matrix. Note that the base state of this extraction is the relative equilibrium.) Since \mathbf{K} is symmetric, see (17), the eigenvalues are real numbers and the eigenvectors form an orthonormal basis of \mathbb{R}^N . Thus,

$$\mathbf{v}_i^\top \mathbf{v}_i = 1 \quad \text{and} \quad \mathbf{v}_i^\top \mathbf{v}_j = 0 \quad \text{for } i \neq j. \quad (22)$$

In other words, the $N \times N$ matrix

$$\mathbf{V} = (\mathbf{v}_1, \mathbf{v}_2, \dots, \mathbf{v}_N) \quad (23)$$

is orthogonal, i. e. $\mathbf{V}^\top = \mathbf{V}^{-1}$. Furthermore, the stiffness matrix diagonalizes under the following operation:

$$\mathbf{V}^\top \mathbf{K} \mathbf{V} = \mathbf{D} = \text{diag}(\lambda_i). \quad (24)$$

The transformation $\mathbf{x} = \mathbf{V}\mathbf{y}$ simply describes a change of basis for vectors in \mathbb{R}^N . We can use it to rewrite the quadratic form (21):

$$F(\mathbf{y}) = \mathbf{y}^\top \mathbf{V}^\top (\mathbf{K} + \mathbf{a}\mathbf{a}^\top) \mathbf{V} \mathbf{y} = \mathbf{y}^\top (\mathbf{V}^\top \mathbf{K} \mathbf{V} + \mathbf{V}^\top \mathbf{a}\mathbf{a}^\top \mathbf{V}) \mathbf{y}$$

Inserting (24) and introducing the vector $\mathbf{b} = \mathbf{V}^\top \mathbf{a}$, which has the components

$$b_i = \mathbf{v}_i^\top \mathbf{a}, \quad (25)$$

this expression is reduced to

$$F(\mathbf{y}) = \mathbf{y}^\top (\mathbf{D} + \mathbf{b}\mathbf{b}^\top) \mathbf{y}. \quad (26)$$

\mathbf{D} is a diagonal matrix containing the eigenvalues of \mathbf{K} and the components of \mathbf{b} are the projections of the vector \mathbf{a} onto the eigenvectors of \mathbf{K} . So our quadratic form is defined by the matrix:

$$\mathbf{B} = \mathbf{D} + \mathbf{b}\mathbf{b}^T = \begin{pmatrix} \lambda_1 + b_1^2 & b_1b_2 & \cdots & b_1b_N \\ b_2b_1 & \lambda_2 + b_2^2 & \cdots & b_2b_N \\ \vdots & \vdots & \ddots & \vdots \\ b_Nb_1 & b_Nb_2 & \cdots & \lambda_N + b_N^2 \end{pmatrix} \quad (27)$$

Now, \mathbf{B} (and therefore \mathbf{A}) is positive definite, if and only if the determinants of all $k \times k$ submatrices,

$$\mathbf{B}_k = \begin{pmatrix} \lambda_1 + b_1^2 & b_1b_2 & b_1b_3 & \cdots & b_1b_k \\ b_2b_1 & \lambda_2 + b_2^2 & b_2b_3 & \cdots & b_2b_k \\ b_3b_1 & b_3b_2 & \lambda_3 + b_3^2 & \cdots & b_3b_k \\ \vdots & \vdots & \vdots & \ddots & \vdots \\ b_kb_1 & b_kb_2 & b_kb_3 & \cdots & \lambda_k + b_k^2 \end{pmatrix}$$

are positive (leading principal minor criterion). In the appendix it is shown, that

$$\det \mathbf{B}_k = \lambda_1 \lambda_2 \cdots \lambda_k \left(1 + \frac{b_1^2}{\lambda_1} + \frac{b_2^2}{\lambda_2} + \cdots + \frac{b_k^2}{\lambda_k} \right). \quad (28)$$

Hence, the relative equilibrium computed from (13) is stable, if $\det \mathbf{B}_k > 0$ for $k = 1, \dots, N$.

5 Fast stability tests

A general stability test for a rotating flexible structure might still be time consuming since *all* eigenvectors and eigenvalues of the tangent stiffness matrix are needed to show that $\det \mathbf{B}_N > 0$. In particular, this could cause difficulties if the structure has many degrees of freedom. In such a case faster tests which enable the stability to be checked without computing $\det \mathbf{B}_k$ from (28) for all $k = 1, \dots, N$ need to be found.

Basically, the sign of $\det \mathbf{B}_k$ is determined by the signs of the eigenvalues $\lambda_1 < \lambda_2 < \cdots < \lambda_N$. Thus, we consider the following cases:

Case 1: $\lambda_1 > 0$

Stability is granted, if λ_1 is positive because then all $\det \mathbf{B}_k$ are positive. For this check, only the lowest eigenvalue of \mathbf{K} must be computed.

Case 2: $\lambda_1 < 0, \lambda_2 < 0$

In this case at least two eigenvalues of \mathbf{K} are negative. Suppose the system is stable, then

$$\det \mathbf{B}_1 = \lambda_1 \left(1 + \frac{b_1^2}{\lambda_1} \right) > 0$$

and since $\lambda_1 < 0$ the bracket must also be negative. Now look at

$$\det \mathbf{B}_2 = \lambda_1 \lambda_2 \left(1 + \frac{b_1^2}{\lambda_1} + \frac{b_2^2}{\lambda_2} \right).$$

Since $\lambda_2 < 0$ the product $\lambda_1 \lambda_2$ is positive and the sign is determined by the bracket. But as seen above $1 + b_1^2/\lambda_1 < 0$. Because also $b_2^2/\lambda_2 < 0$ we obtain $\det \mathbf{B}_2 < 0$. Thus, the system is unstable. For this check, only the first two eigenvalues of \mathbf{K} must be computed.

Case 3: $\lambda_1 < 0, \lambda_2 > 0$

The most complex situation arises, if only one eigenvalue is negative. In this case the factor $\lambda_1 \lambda_2 \dots \lambda_k$ in (28) is negative for all determinants. If $\det \mathbf{B}_k > 0$, also the brackets must be negative:

$$1 + \frac{b_1^2}{\lambda_1} + \frac{b_2^2}{\lambda_2} + \dots + \frac{b_k^2}{\lambda_k} < 0 \quad \text{for } k = 1, \dots, N.$$

On the left side only the term b_1^2/λ_1 is negative by assumption. So the worst case is obtained for $k = N$, where all terms b_i^2/λ_i are added. We may conclude that the system is stable only if

$$1 + \frac{b_1^2}{\lambda_1} + \frac{b_2^2}{\lambda_2} + \dots + \frac{b_N^2}{\lambda_N} = 1 + \sum_{i=1}^N \frac{b_i^2}{\lambda_i} < 0. \quad (29)$$

However, one would prefer an iterative stability test to avoid the computation of all eigenvalues and eigenvectors. In fact, if for any $k < N$

$$1 + \sum_{i=1}^k \frac{b_i^2}{\lambda_i} > 0 \quad (30)$$

the system is *unstable* and the stability test can be stopped at that point. On the other hand, if the sum in (29) is truncated at $i = k$ we can also find an upper limit for the missing terms:

$$\sum_{i=k+1}^N \frac{b_i^2}{\lambda_i} \leq \frac{1}{\lambda_{k+1}} \left(|\mathbf{b}|^2 - \sum_{i=1}^k b_i^2 \right)$$

since $\lambda_{k+1} < \lambda_{k+2} < \dots < \lambda_N$ and $b_{k+1}^2 \leq |\mathbf{b}|^2 - \sum_{i=1}^k b_i^2$. Thus, the system is *stable* if for any $k < N$

$$1 + \sum_{i=1}^k \frac{b_i^2}{\lambda_i} + \frac{1}{\lambda_{k+1}} \left(|\mathbf{b}|^2 - \sum_{i=1}^k b_i^2 \right) < 0 \quad (31)$$

For the tests (30) and (31) only the first $k + 1$ eigenvalues and the first k eigenvectors must be computed. Note that

$$|\mathbf{b}|^2 = |\mathbf{a}|^2$$

since \mathbf{b} is just the decomposition of \mathbf{a} in the orthonormal basis \mathbf{v}_i .

The complete stability test including all cases is depicted in the structogram of fig. 2.

6 Remarks to the finite element method

The complete stability analysis can be carried out with standard FE-software packages. We describe an ABAQUS based approach in this section. In ABAQUS gravitational and centrifugal forces should be included via additional user-elements in order to introduce their correct contribution to the residuum and to the stiffness matrix. Such a user-element is added for every structural finite element.

Basically, the Potential V_G from (10) and the locked inertia tensor M_{cc} from (9) must be expressed by the vector \mathbf{u} of nodal degrees of freedom. This is usually done by subdividing the structure into finite elements. Let $\mathbf{u}^{(e)}$ denote the vector of nodal degrees of freedom for element (e). Then the position \vec{r} of a material point within the element, located at \vec{r}_0 in the reference configuration, is given by

$$\vec{r} = \Psi^{(e)} \mathbf{u}^{(e)} + \vec{r}_0 \quad (32)$$

where $\Psi^{(e)}$ is a linear operator mapping $\mathbf{u}^{(e)} \in \mathbb{R}^{N^{(e)}}$ onto $\vec{r} - \vec{r}_0 \in \mathbb{R}^3$. It is defined by the ansatz-functions used for the discretization process.

If a material point dm is described by a proper density ρ and by an infinitesimal

volumetric interval $d\Omega$ the gravity potential for a finite element reads

$$V_G^{(e)} = \int_{\Omega^{(e)}} \gamma(\vec{r}) d\Omega, \quad \text{where} \quad \gamma(\vec{r}) = -\varrho\kappa \frac{1}{|\vec{r}|} \quad (33)$$

The element residuum is then given by

$$\frac{\partial V_G^{(e)}}{\partial \mathbf{u}^{(e)}} = \int_{\Omega^{(e)}} \boldsymbol{\Psi}^{(e)\top} \vec{g}(\vec{r}) d\Omega, \quad \text{where} \quad \vec{g}(\vec{r}) = \frac{\partial \gamma}{\partial \vec{r}} = -\varrho\kappa \frac{\vec{r}}{|\vec{r}|^3} \quad (34)$$

and the element load stiffness matrix

$$K_{G,ij}^{(e)} = \frac{\partial^2 V_G^{(e)}}{\partial u_i^{(e)} \partial u_j^{(e)}}$$

is

$$\mathbf{K}_G^{(e)} = \int_{\Omega^{(e)}} \boldsymbol{\Psi}^{(e)\top} \mathbf{G}(\vec{r}) \boldsymbol{\Psi}^{(e)} d\Omega, \quad \text{where} \quad \mathbf{G}(\vec{r}) = \frac{\partial \vec{g}}{\partial \vec{r}} = -\frac{\varrho\kappa}{|\vec{r}|^3} \left(3 \frac{\vec{r} \otimes \vec{r}}{|\vec{r}|^2} - \mathbf{I} \right) \quad (35)$$

After numerical integration, (34) and (35) can be coded in the FORTRAN user-subroutine "UEL" provided by ABAQUS. In a similar way the locked inertia tensor may be considered. Altogether, the user elements yield the correct equilibrium equations and the tangent stiffness matrix \mathbf{K} which is needed for the stability test.

7 Examples

7.1 The Space Elevator

To demonstrate an application of the stability test described above we first consider the "space elevator" depicted in fig. 3. For simplicity, the elevator is modeled as homogenous string without bending and torsional stiffness. The modelling space is three-dimensional. Thus, motions out of the orbital plane are taken into account.

For an inextensible string the radial equilibrium configuration, see fig. 3, can be derived directly from Newton's law. Suppose that the system rotates at a given angular rate ω around a celestial body exhibiting the gravitational parameter κ . Furthermore, let L and μ be length and mass per unit length of the string. Introducing R as the orbital radius of the string's mass center we obtain from Newton's second law

$$\mu L R \omega^2 = \int_{R-L/2}^{R+L/2} \frac{\mu \kappa}{r^2} dr = -\mu \kappa \left(\frac{1}{R+L/2} - \frac{1}{R-L/2} \right)$$

yielding

$$\omega^2 = \frac{\kappa}{R^3} \frac{1}{1 - \frac{1}{4} \left(\frac{L}{R}\right)^2} \quad (36)$$

For the subsequent analysis L is increased from $0.1R$ to $1.8R$. Simultaneously, ω is computed from (36), although the string is not completely inextensible in the finite element model. Furthermore, the parameters R , μ and κ are set to unity in order to normalize the problem. To find an appropriate value for the axial stiffness of the string the dimensionless parameter $EAR/(\mu\kappa)$ can be computed for a realistic situation. For example, if the center of mass is in a geostationary orbit around the earth, then $R = 42,000 \text{ km}$ and $\kappa = 3.986 \cdot 10^{14} \text{ m}^3/\text{s}^2$. For a steel string Young's modulus is $E = 2.1 \cdot 10^{11} \text{ N/m}^2$ and the density is given by $\varrho = 7,850 \text{ kg/m}^3$. Thus, since $\mu = \varrho A$, the stiffness parameter would be

$$EA \frac{R}{\mu\kappa} = \frac{ER}{\varrho\kappa} = 3.22.$$

However, in our example the stiffness is increased to 1000.0 in order to approximate the inextensible case.

The result of the stability analysis is explained in fig. 4 and fig. 5. Fig. 4 shows the first two eigenvalues of the tangent stiffness matrix as a function of the string length. Obviously λ_1 is negative and λ_2 is positive in the considered interval. Therefore, case 3 of the stability test discussed in section 5 is relevant here.

As pointed out in section 5 the proof that the system is stable or unstable may require the computation of variable numbers k of eigenvalues. Fig. 5 shows that this number increases along with the string length. At $L \approx 1.0$ thirteen eigenvalues of the tangent stiffness matrix must be evaluated. Beyond $L \approx 1.0$ the system becomes unstable which is proven by the first eigenvalue λ_1 .

This result is in agreement with numerical simulations of the perturbation motions and also with a simplified analytical model of the space elevator. First, fig. 6 shows the perturbation motion of the lower endpoint of the string for a stable and for an unstable configuration. For that purpose a fully dynamic finite element simulation of the string was carried out. It can be observed, that for $L = 0.946R$ (solid line) the point rotates around the earth whereas for $L = 1.018R$ (dashed line) the system descends after a few revolutions. Since both configurations were chosen close to the stability boundary, we may conclude that the stability analysis yielded a reasonable result.

To verify the obtained result we may also derive an analytical stability condition for an inextensible string. According to [(6)] it should be sufficient to consider radial perturbation motions only. Thus, we only have to vary the distance R of the string's mass center in the amended potential.

In the radial configuration shown in fig. 3 the locked inertia tensor according to (9) is simply given by

$$M_{cc} = m \left(R^2 + \frac{L^2}{12} \right),$$

where m denotes the total mass of the string. The potential energy reads

$$V = - \int_{R-L/2}^{R+L/2} \frac{\mu\kappa}{r} dr = -\mu\kappa \ln \frac{R+L/2}{R-L/2}$$

resulting in the amended potential

$$V^*(R) = \frac{p^2}{2M_{cc}(R)} + V(R) \quad (37)$$

where p is the angular momentum of the string. By setting the first derivative of $V^*(R)$ to zero we obtain a relation between the angular momentum and the value of $R = R_0$ at the relative equilibrium:

$$p^2 = \frac{m\kappa\mu}{36} \frac{L}{R_0} \frac{(L^2 + 12R_0^2)^2}{4R_0^2 - L^2}. \quad (38)$$

The stability condition for the inextensible string is then obtained from

$$\left. \frac{d^2V^*}{dR^2} \right|_{R=R_0} > 0 \quad (39)$$

which may be expressed in terms of R_0 by eliminating p using (38). Finally this procedure results in

$$4\kappa\mu \frac{L}{R_0} \frac{L^4 - 48R_0^2L^2 + 48R_0^4}{(L^2 - 4R_0^2)^2(L^2 + 12R_0^2)} > 0.$$

This expression changes its sign if

$$L^4 - 48R_0^2L^2 + 48R_0^4 = 0$$

which happens at $L = 2\sqrt{6 - \sqrt{33}}R_0 \approx 1.01082R_0$. This is in good agreement with the numerical stability test for the orbiting string shown in fig. 5.

7.2 The Orbiting Ring

The second example to be discussed here, is the flexible ring shown in fig. 7. For this structure also bending and torsional stiffness are taken into account.

Again, the problem is treated in three-dimensional space. The basic parameters are selected as follows: Let E be Young's modulus, A the area and J the moment of inertia for bending of the ring's cross section. Assuming a thin walled circular cross section with radius a and thickness h , then

$$A = 2\pi ah \quad \text{and} \quad J = \pi a^3 h.$$

Furthermore, $\mu = \rho A$ denotes the mass per unit length and R the orbital radius of the reference configuration. It is convenient to formulate the problem by means of dimensionless quantities \bar{E} , \bar{A} , \bar{J} , $\bar{\mu}$, $\bar{\kappa}$ and \bar{R} . As for the orbiting string we set $\bar{\mu} = 1$, $\bar{\kappa} = 1$ and $\bar{R} = 1$. To find appropriate values for \bar{E} , \bar{A} and \bar{J} we may consider dimensionless quantities such as

$$\frac{A}{R^2} = \frac{\bar{A}}{\bar{R}^2} = \bar{A}, \quad \frac{J}{R^4} = \frac{\bar{J}}{\bar{R}^4} = \bar{J}$$

$$\frac{ER^3}{\mu\kappa} = \frac{\bar{E}\bar{R}^3}{\bar{\mu}\bar{\kappa}} = \bar{E}$$

Therefore, the dimensionless axial and bending stiffness are given by

$$\bar{E}\bar{A} = \frac{EAR}{\mu\kappa} = \frac{E}{\rho} \frac{R}{\kappa}, \quad \bar{E}\bar{J} = \frac{EJ}{\mu\kappa R} = \frac{E}{\rho} \frac{J}{AR\kappa}.$$

Both expressions do not depend on the wall thickness h of the cross section. However, materials with very high specific Young's modulus E/ρ and a relatively large radius a of the cross section are necessary to avoid complete folding of the ring under the gravitational and centrifugal forces. We choose $R = 42,000 \text{ km}$ and $\kappa = 3.986 \cdot 10^{14} \text{ m}^3/\text{s}^2$ representing a geostationary orbit around the earth, and set $E/\rho = 1.9 \times 10^{10} \text{ Nm/kg}$, which is about 700 times higher than the respective value for steel, yielding $\bar{E}\bar{A} = 2000$. For the cross section radius we assume $a = 0.01R = 420 \text{ km}$ resulting in $\bar{E}\bar{J} = 0.1$. Although these are quite futuristic assumptions compared with today's technology it is interesting to observe the stability behaviour of such structures.

To carry out the stability analysis the angular rate must be defined for the equilibrium. Since we are looking for a geostationary configuration we choose

$$\frac{\omega^2 R^3}{\kappa} = \frac{\bar{\omega}^2 \bar{R}^3}{\bar{\kappa}} = \bar{\omega}^2 = 1.$$

Despite the vast dimensions of the structure the ring deforms significantly under the gravitational and the centrifugal load. Fig. 8 shows the ovalization for varying ring radius $\bar{r} = r/R$. Note that the long axis is pointing towards the center of gravity. The stability analysis shows that the equilibrium is stable up to $\bar{r} \approx 0.4$. As for the orbiting string, λ_1 is negative and λ_2 is positive, see fig. 9. Thus, case 3 of the stability test has to be considered again. For small values of \bar{r} only three eigenvalues are required to show that the system is stable.

However, more eigenvalues must be computed in the vicinity of the stability bound (e. g. 80 at $\bar{r} \approx 0.41$). Beyond the stability bound the proof yields the result from the first eigenvalue. Fig. 10 shows the system at the stability boundary. For the undeformed reference configuration also the dimension of the cross section can be observed. Like in the string-example one may expect that loss of stability affects the overall orbital dynamics and that the system will descend.

Both examples described in this section demonstrate that in many cases the first few eigenvalues and eigenvectors of the tangent stiffness matrix \mathbf{K} are sufficient to obtain information about the stability of an orbiting structure. Furthermore, the test can be integrated efficiently in a finite element analysis with common software packages.

Acknowledgements

I would like to thank my colleagues Klaus Schiefermayr for the fruitful discussions of mathematical questions and Douglas Vaught for improving the linguistic quality of the paper. Furthermore, I thank the reviewers for the helpful comments on the discussion of the examples which were treated more extensively after revision.

APPENDIX: A formula for the determinant of \mathbf{B}_k

By mathematical induction we show that

$$\begin{aligned} \det \mathbf{B}_k &= \det \begin{pmatrix} \lambda_1 + b_1^2 & b_1 b_2 & b_1 b_3 & \cdots & b_1 b_k \\ b_2 b_1 & \lambda_2 + b_2^2 & b_2 b_3 & \cdots & b_2 b_k \\ b_3 b_1 & b_3 b_2 & \lambda_3 + b_3^2 & \cdots & b_3 b_k \\ \vdots & \vdots & \vdots & \ddots & \vdots \\ b_k b_1 & b_k b_2 & b_k b_3 & \cdots & \lambda_k + b_k^2 \end{pmatrix} \\ &= \lambda_1 \lambda_2 \cdots \lambda_k \left(1 + \frac{b_1^2}{\lambda_1} + \frac{b_2^2}{\lambda_2} + \cdots + \frac{b_k^2}{\lambda_k} \right) \end{aligned} \quad (40)$$

where \mathbf{B}_k is the $k \times k$ -matrix introduced in section 4 for the formulation of the stability test.

First, (40) is readily verified for $k = 1$ and $k = 2$. Then we have to show that

(40) is true for any k if it is true for $k - 1$ and $k - 2$. This can be done by simplifying the determinant in the following way.

Provided that $b_{k-1} \neq 0$, multiplying the last row and the last column of \mathbf{B}_k with b_{k-1} yields

$$\det \mathbf{B}_k = \frac{1}{b_{k-1}^2} \det \begin{pmatrix} \lambda_1 + b_1^2 & b_1 b_2 & \cdots & b_1 b_{k-2} & b_1 b_{k-1} & b_1 b_k b_{k-1} \\ b_2 b_1 & \lambda_2 + b_2^2 & \cdots & b_2 b_{k-2} & b_2 b_{k-1} & b_2 b_k b_{k-1} \\ \vdots & \vdots & \ddots & \vdots & \vdots & \vdots \\ b_{k-2} b_1 & b_{k-2} b_2 & \cdots & \lambda_{k-2} + b_{k-2}^2 & b_{k-2} b_{k-1} & b_{k-2} b_k b_{k-1} \\ b_{k-1} b_1 & b_{k-1} b_2 & \cdots & b_{k-1} b_{k-2} & \lambda_{k-1} + b_{k-1}^2 & b_{k-1}^2 b_k \\ b_k b_1 b_{k-1} & b_k b_2 b_{k-1} & \cdots & b_k b_{k-2} b_{k-1} & b_k b_{k-1}^2 & \lambda_k b_{k-1}^2 + b_k^2 b_{k-1}^2 \end{pmatrix}$$

Next we multiply row $k - 1$ with b_k and subtract it from row k :

$$\det \mathbf{B}_k = \frac{1}{b_{k-1}^2} \det \begin{pmatrix} \lambda_1 + b_1^2 & b_1 b_2 & \cdots & b_1 b_{k-2} & b_1 b_{k-1} & b_1 b_k b_{k-1} \\ b_2 b_1 & \lambda_2 + b_2^2 & \cdots & b_2 b_{k-2} & b_2 b_{k-1} & b_2 b_k b_{k-1} \\ \vdots & \vdots & \ddots & \vdots & \vdots & \vdots \\ b_{k-2} b_1 & b_{k-2} b_2 & \cdots & \lambda_{k-2} + b_{k-2}^2 & b_{k-2} b_{k-1} & b_{k-2} b_k b_{k-1} \\ b_{k-1} b_1 & b_{k-1} b_2 & \cdots & b_{k-1} b_{k-2} & \lambda_{k-1} + b_{k-1}^2 & b_{k-1}^2 b_k \\ 0 & 0 & \cdots & 0 & -\lambda_{k-1} b_k & \lambda_k b_{k-1}^2 \end{pmatrix}$$

Performing the same operation with columns $k - 1$ and k leads to

$$\det \mathbf{B}_k = \frac{1}{b_{k-1}^2} \det \begin{pmatrix} \lambda_1 + b_1^2 & b_1 b_2 & \cdots & b_1 b_{k-2} & b_1 b_{k-1} & 0 \\ b_2 b_1 & \lambda_2 + b_2^2 & \cdots & b_2 b_{k-2} & b_2 b_{k-1} & 0 \\ \vdots & \vdots & \ddots & \vdots & \vdots & \vdots \\ b_{k-2} b_1 & b_{k-2} b_2 & \cdots & \lambda_{k-2} + b_{k-2}^2 & b_{k-2} b_{k-1} & 0 \\ b_{k-1} b_1 & b_{k-1} b_2 & \cdots & b_{k-1} b_{k-2} & \lambda_{k-1} + b_{k-1}^2 & -\lambda_{k-1} b_k \\ 0 & 0 & \cdots & 0 & -\lambda_{k-1} b_k & \lambda_k b_{k-1}^2 + \lambda_{k-1} b_k^2 \end{pmatrix}$$

Involving the determinants of \mathbf{B}_{k-1} and \mathbf{B}_{k-2} we can expand $\det \mathbf{B}_k$ from the last row:

$$\begin{aligned}\det \mathbf{B}_k &= \frac{1}{b_{k-1}^2} \left[(\lambda_k b_{k-1}^2 + \lambda_{k-1} b_k^2) \det \mathbf{B}_{k-1} + \lambda_{k-1} b_k (-\lambda_{k-1} b_k) \det \mathbf{B}_{k-2} \right] \\ &= \frac{b_k^2}{b_{k-1}^2} \lambda_{k-1} \left[\det \mathbf{B}_{k-1} - \lambda_{k-1} \det \mathbf{B}_{k-2} \right] + \lambda_k \det \mathbf{B}_{k-1}\end{aligned}$$

If we now substitute the induction hypothesis for $\det \mathbf{B}_{k-1}$ and $\det \mathbf{B}_{k-2}$

$$\begin{aligned}\det \mathbf{B}_{k-1} &= \lambda_1 \lambda_2 \dots \lambda_{k-1} \left(1 + \frac{b_1^2}{\lambda_1} + \frac{b_2^2}{\lambda_2} + \dots + \frac{b_{k-1}^2}{\lambda_{k-1}} \right) \\ \det \mathbf{B}_{k-2} &= \lambda_1 \lambda_2 \dots \lambda_{k-2} \left(1 + \frac{b_1^2}{\lambda_1} + \frac{b_2^2}{\lambda_2} + \dots + \frac{b_{k-2}^2}{\lambda_{k-2}} \right)\end{aligned}$$

we conclude that

$$\begin{aligned}\det \mathbf{B}_k &= \frac{b_k^2}{b_{k-1}^2} \lambda_{k-1} \left[\lambda_1 \lambda_2 \dots \lambda_{k-1} \frac{b_{k-1}^2}{\lambda_{k-1}} \right] \\ &\quad + \lambda_1 \lambda_2 \dots \lambda_k \left(1 + \frac{b_1^2}{\lambda_1} + \frac{b_2^2}{\lambda_2} + \dots + \frac{b_{k-1}^2}{\lambda_{k-1}} \right) \\ &= \lambda_1 \lambda_2 \dots \lambda_k \left(1 + \frac{b_1^2}{\lambda_1} + \frac{b_2^2}{\lambda_2} + \dots + \frac{b_k^2}{\lambda_k} \right).\end{aligned}$$

This is exactly the hypothesis for $\det \mathbf{B}_k$ which is therefore proved. Since we have supposed $b_{k-1} \neq 0$ for our proof we finally must consider the situation where some b_i are zero. However, in this case the matrix \mathbf{B}_k can be rearranged by exchanging rows and columns so that all elements with non-zero b_i are collected in the upper left corner of the matrix. Now let $\bar{b}_1, \dots, \bar{b}_m$ denote the sequence of all non-zero b_i appearing in \mathbf{B}_k and let $\bar{\lambda}_1, \dots, \bar{\lambda}_m$ be the corresponding sequence of λ_i ($m \leq k$). Then by exchanging rows and columns we obtain

$$\det \mathbf{B}_k = \det \begin{pmatrix} \bar{\lambda}_1 + \bar{b}_1^2 & \bar{b}_1 \bar{b}_2 & \dots & \bar{b}_1 \bar{b}_k & 0 & \dots & 0 \\ \bar{b}_2 \bar{b}_1 & \bar{\lambda}_2 + \bar{b}_2^2 & \dots & \bar{b}_2 \bar{b}_k & 0 & \dots & 0 \\ \vdots & \vdots & \ddots & \vdots & \vdots & \vdots & \vdots \\ \bar{b}_m \bar{b}_1 & \bar{b}_m \bar{b}_2 & \dots & \bar{\lambda}_m + \bar{b}_m^2 & 0 & \dots & 0 \\ 0 & 0 & \dots & 0 & \bar{\lambda}_{m+1} & \dots & 0 \\ \vdots & \vdots & \vdots & \vdots & \vdots & \ddots & \vdots \\ 0 & 0 & \dots & 0 & 0 & \dots & \bar{\lambda}_k \end{pmatrix}$$

Clearly, this determinant is given by

$$\det \mathbf{B}_k = \bar{\lambda}_{m+1} \dots \bar{\lambda}_k \det \begin{pmatrix} \bar{\lambda}_1 + \bar{b}_1^2 & \bar{b}_1 \bar{b}_2 & \dots & \bar{b}_1 \bar{b}_k \\ \bar{b}_2 \bar{b}_1 & \bar{\lambda}_2 + \bar{b}_2^2 & \dots & \bar{b}_2 \bar{b}_k \\ \vdots & \vdots & \ddots & \vdots \\ \bar{b}_m \bar{b}_1 & \bar{b}_m \bar{b}_2 & \dots & \bar{\lambda}_m + \bar{b}_m^2 \end{pmatrix}$$

For the remaining determinant we may already use our hypothesis since per definition $\bar{b}_i \neq 0$. Introducing the sequence of zero b_i 's by $\bar{b}_{m+1}, \dots, \bar{b}_k = 0$ we obtain

$$\det \mathbf{B}_k = \bar{\lambda}_{m+1} \dots \bar{\lambda}_k \bar{\lambda}_1 \dots \bar{\lambda}_m \left(1 + \frac{\bar{b}_1^2}{\bar{\lambda}_1} + \dots + \frac{\bar{b}_m^2}{\bar{\lambda}_m} + \frac{\bar{b}_{m+1}^2}{\bar{\lambda}_{m+1}} + \dots + \frac{\bar{b}_k^2}{\bar{\lambda}_k} \right)$$

In this expression the sequence is irrelevant and we may omit the bars yielding again the formula for $\det \mathbf{B}_k$. Thus, our proof is complete.

References

- [1] BELETSKY, V. V., LEVIN, E. M. *Dynamics of Space Tether Systems*, Advances of the Astronautical Sciences, Vol. 83 (1993), San Diego, CA: AAS Publication Office.
- [2] KRUPA, M., SCHAGERL, M., STEINDL, A., TROGER, H. *Stability of Relative Equilibria. Part I: Comparison of Four Methods*, Meccanica 35 (2001) 325-351, Kluwer Academic Publishers.
- [3] KRUPA, M., STEINDL, A., TROGER, H. *Stability of Relative Equilibria. Part II: Dumbell Satellites*, Meccanica 35 (2001) 353-371, Kluwer Academic Publishers.
- [4] MARSDEN, J. E., RATIU, T. S. *An introduction to Mechanics and Symmetry, A Basic Exposition of Classical Mechanical Systems*, Springer - Verlag, New York, Heidelberg, Berlin, 1994.
- [5] SIMO, J. C., POSBERGH, T. A., MARSDEN, J. E. *Stability of Relative Equilibria. Part I: The reduced energy-momentum method*, Arch. Rat. Mech. Anal. 115 (1991a) 15-59.
- [6] STEINDL, A., TROGER, H. *Is the Sky-Hook Configuration Stable?*, Non-linear Dynamics 40 (2005) 419-431.
- [7] STEINER, W. *Stability Analysis of Relative Equilibria of Mechanical Systems with Cyclic Coordinates: A Direct Approach*, Arch. Appl. Mech. 75 (2006) 355-363.

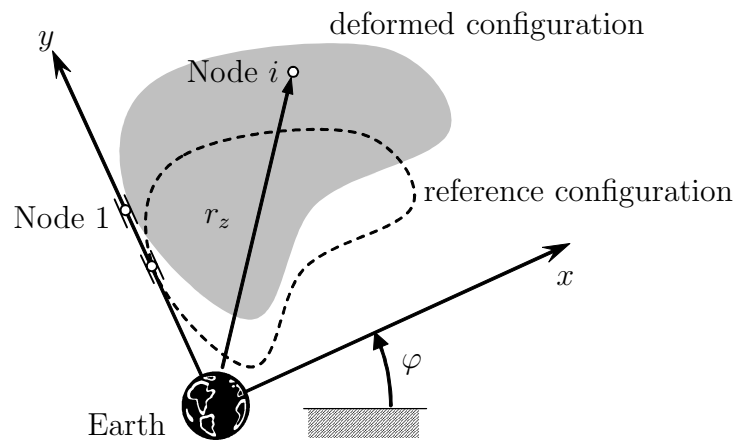


Fig. 1. A flexible orbiting structure in a rotating reference frame.

Accepted manuscript

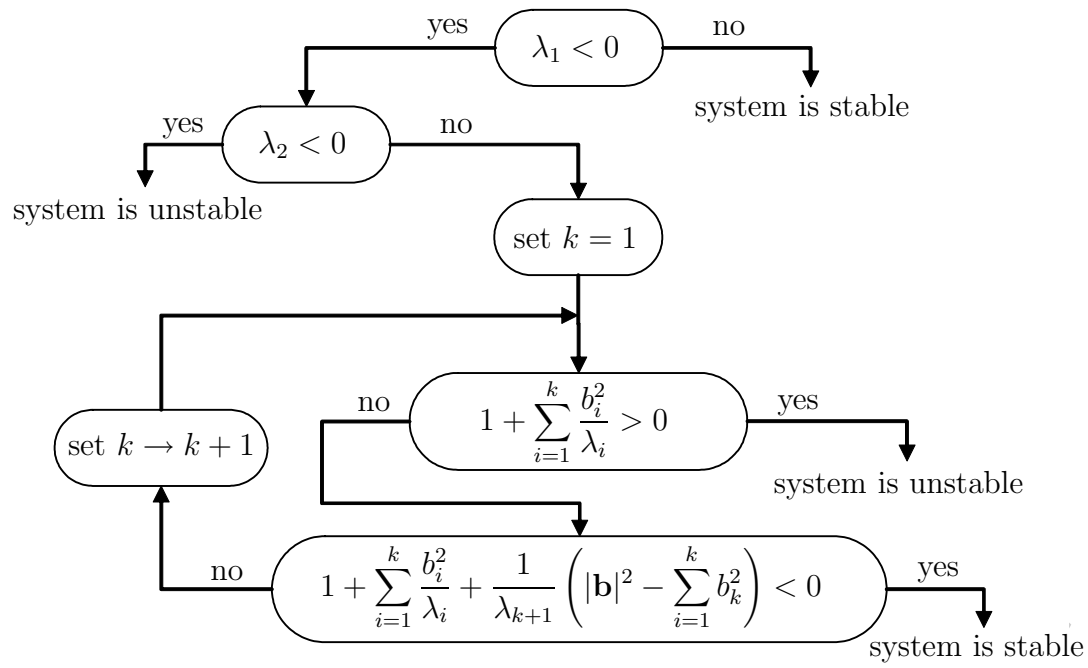


Fig. 2. Structogram of the stability testing process.

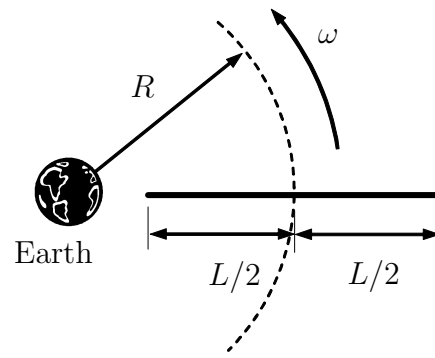


Fig. 3. The orbiting string.

Accepted manuscript

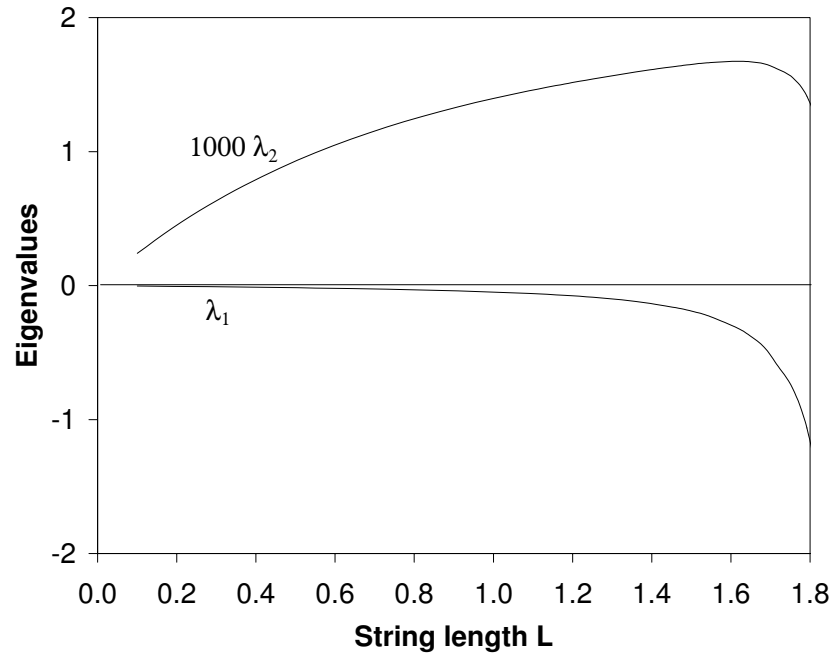


Fig. 4. First eigenvalues of the orbiting string for varying length L .

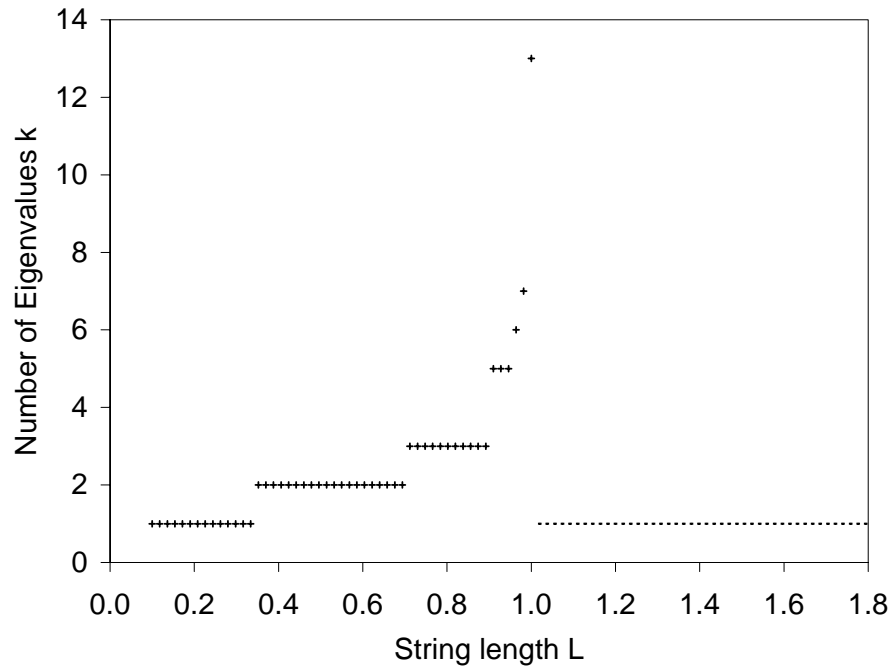


Fig. 5. Number of eigenvalues and eigenvectors of the orbiting string needed for the stability test.

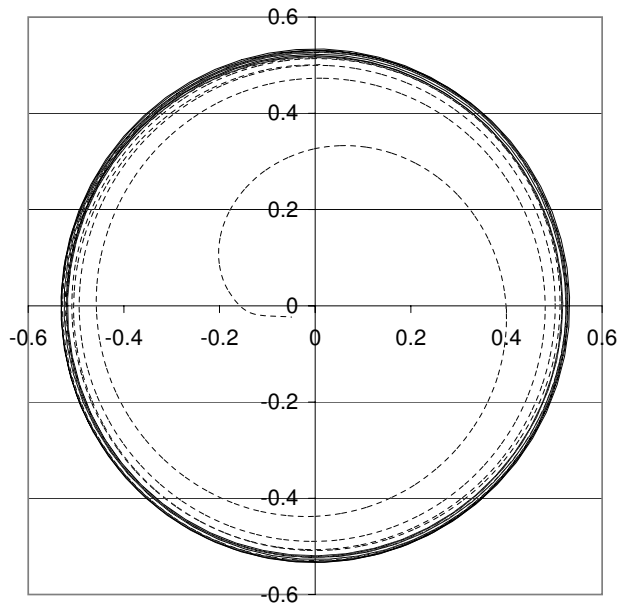


Fig. 6. Two orbits of the lower end point of the string from fig. 3 after slight perturbations of the radial equilibria. For $L = 0.946R$ (solid line) the equilibrium is stable whereas for $L = 1.018R$ (dashed line) the the equilibrium has become unstable.

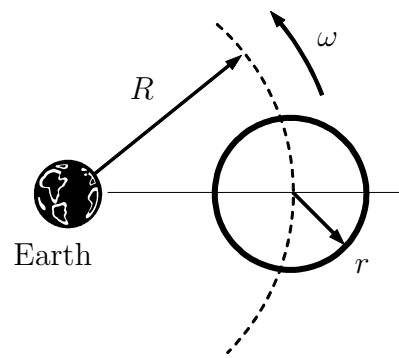


Fig. 7. The orbiting ring.

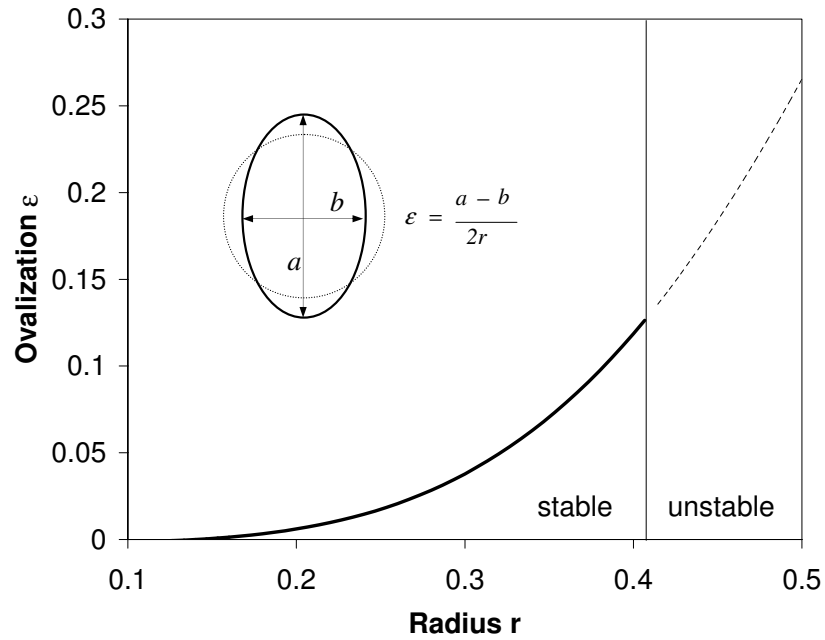


Fig. 8. Ovalization of the orbiting ring for varying radius \bar{r} . The system is stable up to $\bar{r} \approx 0.4$.

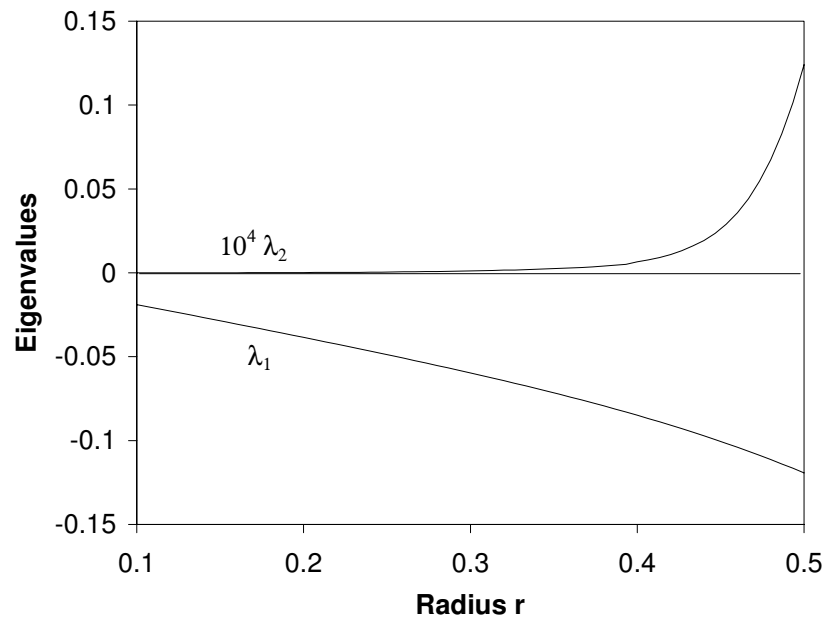


Fig. 9. First eigenvalues of the orbiting ring for varying radius \bar{r} .

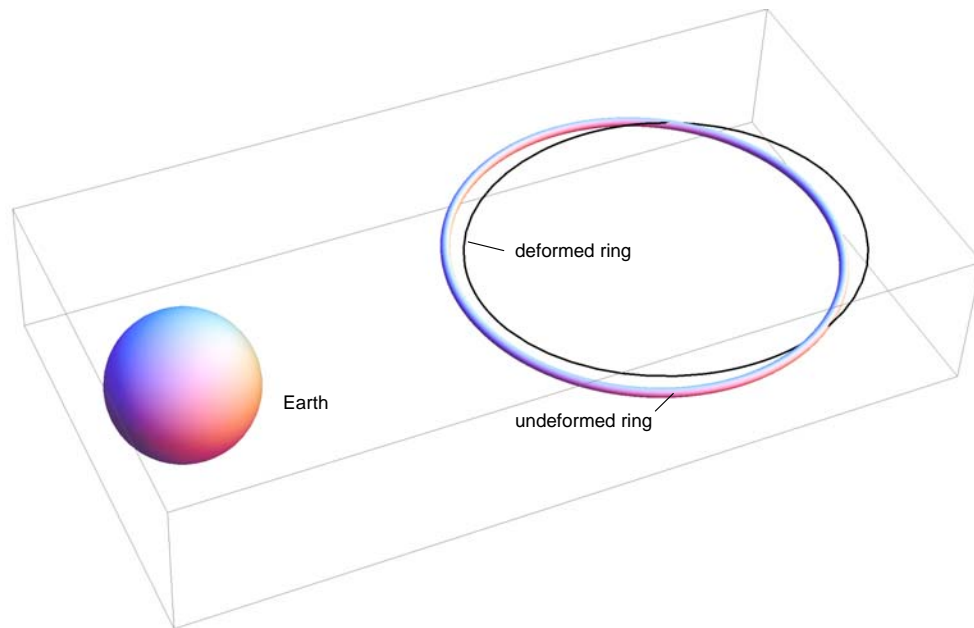


Fig. 10. Deformed and undeformed shape of the orbiting ring at the stability boundary.